Optimization of the cathode material for nitrate removal by a paired electrolysis process

David Reyter [a,b], Daniel Bélanger [b], Lionel Roué [a,*]

[a] INRS Energie, Matériaux et Télécommunications, 1650 bd. Lionel-Boulet, Varennes (QC), J3X 1S2, Canada
[b] Département de Chimie, UQAM, CP 8888, Montréal (QC), H3C 3P8, Canada

ABSTRACT

Ni, Cu, $Cu_{90}Ni_{10}$ and $Cu_{70}Ni_{30}$ were evaluated as cathode materials for the conversion of nitrate to nitrogen by a paired electrolysis process using an undivided flow-through electrolyzer. Firstly, corrosion measurements revealed that Ni and $Cu_{70}Ni_{30}$ electrodes have a much better corrosion resistance than Cu and $Cu_{90}Ni_{10}$ in the presence of chloride, nitrate and ammonia. Secondly, nitrate electroreduction experiments showed that the cupro-nickel electrodes are the most efficient for reducing nitrate to ammonia with a selectivity of 100%. Finally, paired electrolysis experiments confirmed the efficiency of $Cu_{70}Ni_{30}$ and $Cu_{90}Ni_{10}$ cathodes for the conversion of nitrate to nitrogen. During a typical electrolysis, the concentration of nitrate varied from 620 ppm to less than 50 ppm NO_3^- with an N_2 selectivity of 100% and a mean energy consumption of 20 kWh/kg NO_3^- (compared to ~35 and ~220 kWh/kg NO_3^- with Cu and Ni cathodes, respectively).
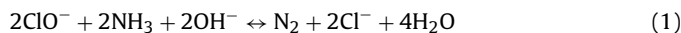
1. Introduction

Nitrate (NO_3^-) contamination in ground and surface water is a growing environmental worldwide concern. It mainly results from the excessive use of synthetic nitrogen fertilizers and livestock manure in intensive agriculture and, to a lesser extent, to the discharge of industrial and municipal effluents. Nitrate pollution can cause serious problems on aquatic ecosystems (e.g., eutrophication) and on human health (e.g., gastrointestinal cancer) [1–3]. The World Health Organization recommends a maximum limit of 45 mg L^{-1} of nitrate in drinking water [4].

Currently, the nitrate remediation processes predominantly used are ion exchange and biological denitrification. Membrane separation processes such as electrodialysis reversal and reverse osmosis can also be used for nitrate removal. Unfortunately, these processes show some drawbacks (e.g., continuous monitoring, slow kinetics, generation of byproducts). In this context, the electrochemical approach is receiving more and more attention due to its convenience, ability to treat highly concentrated nitrate or bactericide effluents, low investment cost and environmental friendliness, particularly if the resulting product is harmless nitrogen [5].

Nitrate electroreduction has been widely studied [6,7] with several monometallic electrodes such as Pb, Ni, Zn [8,9] or Rh, Ru, Ir, Pd, Cu, Ag, Au [10–16]. Among these materials, copper is known as the

best promoter for nitrate electroreduction by producing ammonia and nitrite [12,13] depending on the electrode potential. Bimetallic Cu–Pd electrodes also showed interesting electrocatalytic properties with a good selectivity toward nitrate electroreduction to nitrogen [17–19]. However, the Pd/Cu surface ratio and the electrode potential have to be accurately controlled otherwise nitrite or ammonia will be produced. Moreover, under these conditions, the nitrate destruction rate remained very slow [17].

On the other hand, electrochemical oxidation of ammonia has been studied on dimensionally stable anodes (DSAs) [20–23]. In the presence of chloride, chlorine is generated at the anode and immediately transformed to hypochlorite, which reacts with ammonia to produce nitrogen in alkaline media according to the reaction:

$$2ClO^- + 2NH_3 + 2OH^- \leftrightarrow N_2 + 2Cl^- + 4H_2O \qquad (1)$$

Recently, the simultaneous reduction of the nitrate and the oxidation of the produced ammonia has been investigated in various cell configurations [24–29]. This paired electrolysis approach seems to be the most efficient electrochemical method for converting the nitrate to nitrogen. Ideally, it should be performed by using an undivided cell reactor (i.e., without membrane) in order to avoid the problems associated with membrane degradation (e.g., blocking by carbonates or organic compounds). In this context, the main difficulty is to find the proper conditions to perform both the reduction of the nitrate to ammonia and the oxidation of ammonia to nitrogen. To date, copper is preferred as cathode material because of its good activity for nitrate electroreduction [30]. However, at a pure copper cathode, nitrite is generated in addition to ammonia.

* Corresponding author. Tel.: +1 450 929 8185; fax: +1 450 929 8102.
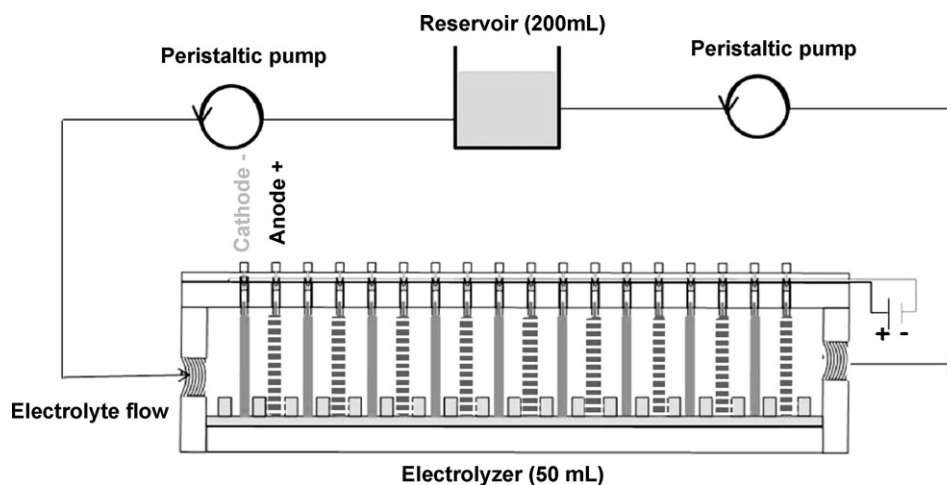*E-mail address:* roue@emt.inrs.ca (L. Roué).

Fig. 1. Schematic representation of the multi-cell electrolyzer.

In an undivided cell, nitrite ions can be oxidized to nitrate at the anode, strongly decreasing the efficiency of the paired electrolysis [31]. Another limitation of copper is its poor corrosion resistance in presence of chloride, nitrate and ammonia [32].

The aim of this study was to investigate new candidates as cathodes for nitrate removal by paired electrolysis in an undivided cell. Cupro-nickel materials were selected because of their well-known good corrosion resistance in salt water. Moreover, nickel has a good electroactivity for hydrogenation while copper displays a good activity for nitrate electroreduction. As a result, a synergistic effect of alloying Ni with Cu could be expected, enhancing the conversion of nitrate to ammonia [33].

Firstly, the corrosion resistance of copper–nickel based electrodes was studied in the presence of chloride, nitrate and ammonia. Then, their activity and selectivity toward ammonia generation during nitrate electroreduction were evaluated. Finally, they were tested as cathode materials for nitrate removal in a paired electrolysis process using an undivided cell with a DSA electrode as anode. Pure copper and nickel cathodes were also tested for comparison.

2. Experimental

2.1. Electrode materials

Four commercial metals were studied as cathodes: copper (99.5%), nickel (99.5%), Cu:Ni 70:30 wt.% (C71500) and Cu:Ni 90:10 wt.% (C70600). The surfaces were abraded with fine emery paper and polished with alumina powder down to 1 μm and finally rinsed with distilled water. Commercial Ti/IrO$_2$ grids (Ti Anode Fabricators Pvt. Ltd.) were used as anodes.

2.2. Electrochemical measurements

All experiments were performed in alkaline media (pH 12) for the following reasons: (i) during nitrate electroreduction, OH$^-$ anions are generated and thus, by choosing an initial pH of 12, the variation of the pH upon experiments is limited; (ii) at pH 12, ammonia is essentially in the form of NH$_3$ (pK_a NH$_4{}^+$/NH$_3$ = 9.2), which is favorable for its conversion to nitrogen [22]; (iii) at pH 12, chloramines production resulting from the oxidation of ammonia by hypochlorite is prevented [38]. In addition, all experiments were performed at room temperature and no significant evolution of the electrolyte temperature was observed during the experiments.

Polarization tests were conducted in a single compartment glass cell containing a Pt counter electrode with an external saturated calomel reference electrode (SCE) interfaced to the electrolyte via a Luggin capillary. The geometric surface area of the working electrode was 4 cm^2. In all cases, the supporting electrolyte was a 0.5 M NaCl + 0.01 M NaOH (pH 12) aqueous solution. During the evaluation of the electrodes for corrosion resistance or nitrate reduction, the appropriate amount of NaNO$_3$ or NH$_4$Cl was added to the electrolyte. Before each test, dissolved oxygen was removed from the solution by bubbling with high-purity argon for 20 min. In addition, sample surfaces were examined by optical microscopy (LV100 microscope, Nikkon Eclipse) after immersion for 3 days in open circuit conditions in 0.5 M NaCl + 0.01 M NaOH in presence or not of 0.01 M NaNO$_3$ or 0.01 M NH$_4$Cl.

Prolonged nitrate electroreduction tests were performed for 24 h at −1.3 V vs. SCE for pure copper and at −1.1 V vs. SCE for pure nickel and cupro-nickel cathodes. A two-compartment cell made of borosilicate glass and separated by a cation-exchange membrane (Nafion 117) was used (see its schematic representation in [33]). The cathodic compartment contained the working electrode (S = 4 cm^2), a Luggin capillary linked to an SCE reference electrode, and 150 mL of 0.01 M NaOH + 0.5 M NaCl + 0.1 M NaNO$_3$ solution. The anodic compartment contained a platinum wire as counter-electrode in a 0.01 M NaOH + 0.5 M NaCl solution. Before the experiments, the cathodic compartment was purged with Ar for 30 min and then sealed to avoid the release of formed gases (e.g., H$_2$, N$_2$, N$_2$O) and a manometer was used to measure the pressure.

Paired electrolyses were done using a multi-cell electrolyzer without a membrane in semi batch mode (Fig. 1). The flow rate (200 mL min^{-1}) was controlled by two peristaltic pumps. A total of 9 anode grids and 9 cathode plates of 8 cm^2 each (geometric surface area) are alternatively placed face to face with an interelectrode spacing of 4 mm. The volume of the effluent tank is 200 mL, while that of the electrolyzer is 50 mL. Potentiostatic electrolyses were controlled by using a VMP3 multichannel potentiostat/galvanostat (BioLogic Science Instruments).

2.3. Chemical analyses

After each electrolysis, the NH$_3$ concentration was determined by visible spectroscopy (Nessler's method) on a Varian spectrometer (Cary-1E). Gas chromatographic analyses of N$_2$, Ar, H$_2$ and N$_2$O were performed on a Varian 3000 gas chromatograph (molecular sieve 5 Å and 200 cm × 0.3 cm). The concentrations of NO$_3{}^-$, NO$_2{}^-$ and Cl$^-$ anions were measured by an ion chromatograph (Dionex 1500) equipped with a Dionex Ion Pac AS14A Anion Exchange column and a chemical suppressor (ASR-ultra 4 mm), using 8 mM Na$_2$CO$_3$ + 1 mM NaHCO$_3$ as eluent at 1 mL min^{-1}.

The electrode performance for nitrate removal was evaluated using the following criteria:

- nitrate destruction or conversion yield (%) defined as $(C_0 - C_t)/C_0 \times 100$ where C_0 and C_t are the nitrate concentrations at the beginning and at the end of the electrolysis, respectively.
- selectivity $S(j)$ (%) of nitrate reduction to a nitrogen-containing product j defined as $m_j \times 100/\sum m$, where m_j the quantity of product j and $\sum m$ the sum of all nitrogen-containing products.
- current efficiency CE (%) of the paired electrolysis process, which is calculated on the basis of the cathodic current efficiency since the reduction of nitrate to ammonia requires more electrons than for the oxidation of ammonia to nitrogen. It is defined as $(n_{NO_3^-} \times 8 \times F) \times 100/q$ where $n_{NO_3^-}$ is the number of converted NO_3^- moles, q the total electrical charge (C) consumed during the electrolysis and F the Faraday constant (96485 C mol^{-1}) and considering that 8 electrons are involved in the reduction of nitrate to ammonia.

3. Results and discussion

3.1. Corrosion resistance

The corrosion behavior of Cu, Cu$_{90}$Ni$_{10}$, Cu$_{70}$Ni$_{30}$ and Ni was investigated in an alkaline chloride solution (0.5 M NaCl, pH 12) in the presence of 10 mM NaNO$_3$ and 10 mM NH$_4$Cl. From potentiodynamic polarization curves (Fig. 2), the values of the corrosion potential E_{corr}, pitting potential E_p and corrosion current density i_{corr} were determined (Table 1).

Polarization curves of these electrodes in a 0.5 M NaCl solution at pH 12 are shown in Fig. 2a. There are different active regions for copper. The first peak near 0.0 V is attributed to the formation of Cu$_2$O. The second wave at 0.1 V is assigned to the conversion of the outer layer of the Cu$_2$O to CuO/Cu(OH)$_2$ [34]. By comparing the different curves in Fig. 2a, it appears that the current density measured in the anodic zone decreases with increasing nickel content. For all electrodes, the breakdown of the passivity is marked by a sharp increase of the current density and the appearance of a current loop after the potential scan reversal (not shown). For a pure copper electrode, the potential range of passivity is very limited since film breakdown occurs at ca. 200 mV, reflecting the poor passive behavior of Cu(OH)$_2$ in the presence of chloride. The electrode corrosion resistance increases with the nickel content (Table 1) due to the formation of a Ni(OH)$_2$ passive layer [35].

In the presence of nitrate (Fig. 2b), the passive behavior for Cu and Cu–Ni electrodes is more pronounced, as illustrated by a wider passive region, a nobler breakdown potential and a lower corrosion current (Table 1). In contrast, the presence of ammonia (Fig. 2c and Table 1) has a detrimental effect on the corrosion resistance of the copper and cupro-nickel materials. The pitting potential of Cu decreases from 200 to 55 mV and its corrosion current increases from 4.7 to 10.4 mA cm^{-2} with ammonia addition. Actually, in the presence of ammonia, the copper oxide layer is destabilized by the formation of the soluble [Cu(NH$_3$)$_6$]$^{2+}$ complex [36,37]. For pure nickel and cupro-nickel electrodes, NH$_3$ with chloride produce various soluble complexes (e.g., NiCl$_2$(NH$_3$)$_4$, [Ni(H$_2$O)$_5$NH$_3$]$^{2+}$) which can lead to a general or localized corrosion [36,37]. However, pure nickel and Ni–Cu alloys remain much more resistant to corrosion than copper with one order of magnitude lower corrosion current density (Table 1).

Fig. 3 shows optical micrographs of the samples immersed for 3 days in 0.5 M NaCl at pH 12 (a) and in the same solution with the addition of 10 mM NaNO$_3$ (b) or 10 mM NH$_4$Cl (c). These micrographs confirm that the corrosion resistance of the investigated
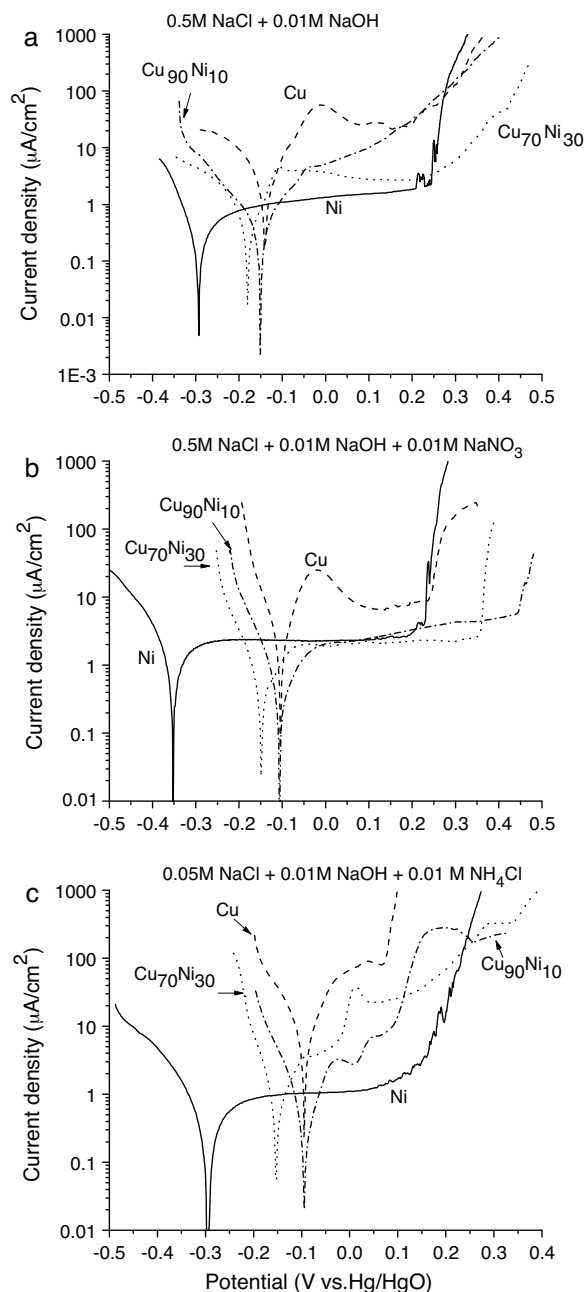

Fig. 2. Polarization curves of Cu, Cu$_{90}$Ni$_{10}$, Cu$_{70}$Ni$_{30}$ and Ni electrodes in 0.01 M NaOH + 0.5 M NaCl (a) and in the presence of 0.01 M NaNO$_3$ (b) or 0.01 M NH$_3$ (c). Scan rate: 0.166 mV s^{-1}.

materials increases with their nickel content. As expected, copper shows the most corroded surface in all three media. The Cu$_{90}$Ni$_{10}$ alloy is mainly affected by the addition of ammonia, producing a bundle of pits approximately 10 μm diameter on its surface. On the other hand, Cu$_{70}$Ni$_{30}$ and pure nickel present a limited corrosion in the presence of chloride, nitrate or ammonia. Their surfaces only present a few tiny pits surrounded by corrosion products.

3.2. Electrochemical behavior of the cathode materials for nitrate reduction

Fig. 4 shows linear sweep voltammograms (LSVs) recorded for pure nickel, pure copper and cupro-nickel electrodes in 0.5 M NaCl + 0.01 M NaOH with or without nitrate. LSVs of Cu and Ni electrodes without nitrate (dotted curves) show only background

Table 1
Corrosion potential (E_{corr}), corrosion current (i_{corr}) and pitting potential (E_p) determined from polarization curves of Cu, Ni, $Cu_{70}Ni_{30}$ and $Cu_{90}Ni_{10}$ alloys in different media.

	0.5 M NaCl + 0.01 M NaOH			0.5 M NaCl + 0.01 M NaOH + 0.01 M NaNO$_3$			0.5 M NaCl + 0.01 M NaOH + 0.01 M NH$_4$Cl		
	E_{corr} (mV)	i_{corr} (mA cm^{-2})	E_p (mV)	E_{corr} (mV)	i_{corr} (mA cm^{-2})	E_p (mV)	E_{corr} (mV)	i_{corr} (mA cm^{-2})	E_p (mV)
Cu	−141	4.7	200	−93	4.4	225	−103	10.4	55
$Cu_{90}Ni_{10}$	−149	1.6	241	−97	0.9	450	−117	1.2	100
$Cu_{70}Ni_{30}$	−180	1.1	250	−139	1.1	350	−159	1.4	252
Ni	−293	0.7	241	−354	0.91	220	−295	1.1	150
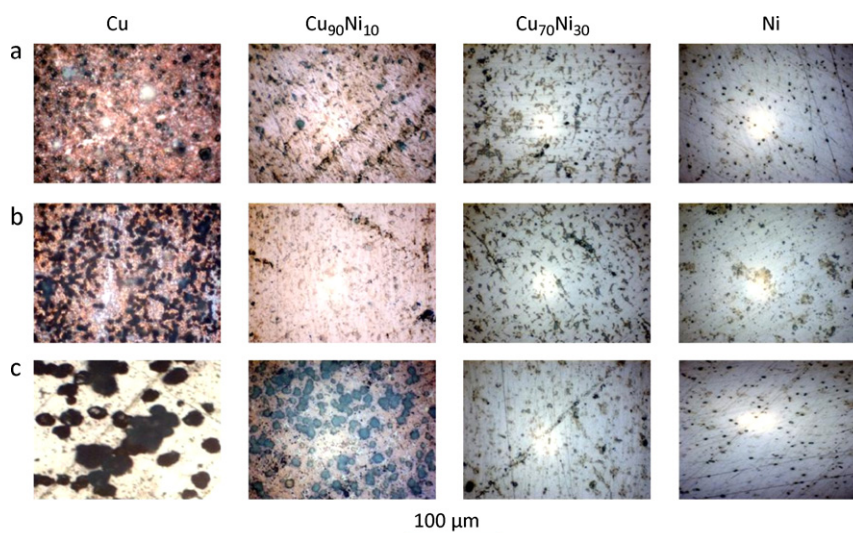
Fig. 3. Optical micrographs of Cu, $Cu_{90}Ni_{10}$, $Cu_{70}Ni_{30}$ and Ni surfaces after immersion for 72 h in 0.5 M NaCl + 0.01 M NaOH (a) and in the presence of 0.01 M NaNO$_3$ (b) or 0.01 M NH$_4$Cl (c).

current prior to an abrupt increase of the cathodic current due to the hydrogen evolution reaction (HER) at a potential lower than −1.4 and −1.1 V, respectively. The LSV of the copper electrode in the presence of nitrate shows two reduction waves. The first one at −1.1 V is attributed to the reduction of nitrate to nitrite, and the second one at −1.3 V is assigned to the reduction of nitrite to ammonia [13]. LSVs recorded in the presence of nitrate for pure nickel and cupro-nickel electrodes show an onset of the cathodic current at about −0.85 V and a maximum is reached at about −1.15 V just before the onset of the hydrogen evolution reaction. Prolonged electrolyses demonstrate that this wave is attributed to the reduc-
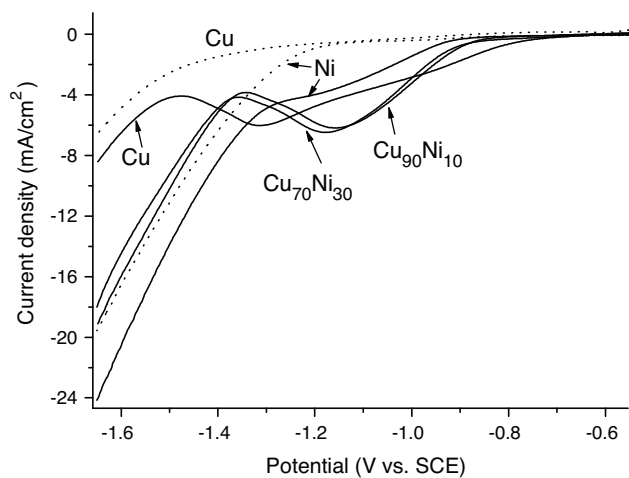
tion of nitrate to ammonia (see below). The logarithmic plots (not shown) of the current density for nitrate reduction measured at −1.25 V from the LSV curves as a function of the nitrate concentration (from 10 to 30 mM) yield a straight line according to the equation:

$$\log i_{-1.25V} = \log k + n \log[NO_3^-] \tag{2}$$

where k is the reaction rate constant and n the reaction order. All the electrodes present a reaction order close to 1. The rate constants for nitrate reduction using the $Cu_{90}Ni_{10}$ ($k \approx 0.43$ s^{-1}) and $Cu_{70}Ni_{30}$ ($k \approx 0.46$ s^{-1}) electrodes are much higher than that of the Cu electrode ($k \approx 0.26$ s^{-1}), confirming that nitrate electroreduction is more effective for the cupro-nickel electrodes. The rate constant for nitrate reduction on the pure nickel electrode is even smaller ($k \approx 0.18$ s^{-1}).

3.3. Electrolysis with a two-compartment cell

In order to identify and quantify the nitrate-reduction products, prolonged electrolyses of a solution containing 0.01 M NaNO$_3$ in 0.5 M NaCl + 0.01 M NaOH were carried out at −1.3 V for the copper electrode and −1.1 V for the nickel and cupro-nickel electrodes, i.e., at potential where the activity of each electrode is maximum for nitrate electroreduction on the basis of the previous LSV curves (Fig. 4). Fig. 5a–d displays the evolution of the N-concentration (ppm) of nitrate and reaction products formed during these electrolyses for the different cathode materials. Ammonia and nitrite were the only nitrate-reduction products detected in the solution and no N-containing gas was detected at these potentials. The nitrate destruction rate depends on the cathode used for the electrolysis. It is also clearly apparent that the selectivity for nitrite or ammonia is strongly influenced by the cathode material. As expected, copper has a good activity for nitrate electroreduction
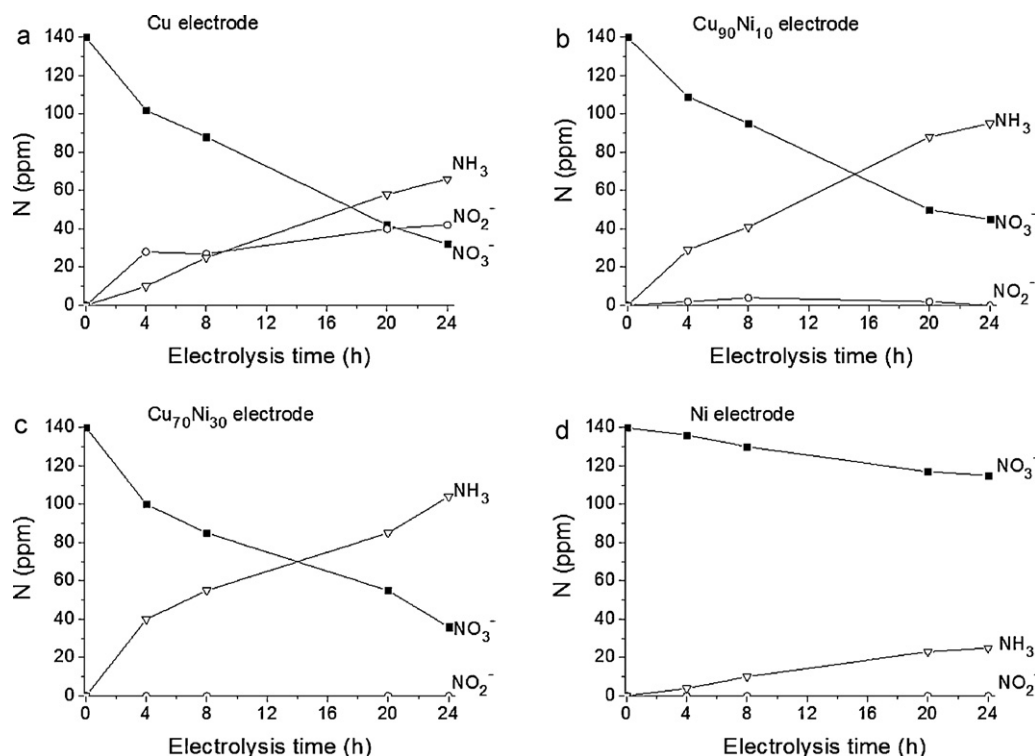

Fig. 4. Linear sweep voltammograms of Cu, $Cu_{90}Ni_{10}$, $Cu_{70}Ni_{30}$ and Ni electrodes in 0.5 M NaCl + 0.01 M NaOH (dotted curves for Ni and Cu) in the presence of 0.01 M NaNO$_3$ (solid curves). Scan rate: 20 mV s^{-1}.

Fig. 5. Evolution of the nitrate, nitrite and ammonia concentrations during a 24 h electrolysis of 0.01 M NaNO$_3$ in 0.5 M NaCl + 0.01 M NaOH at −1.3 V with a Cu (a) and at −1.1 V with Cu$_{90}$Ni$_{30}$ (b), Cu$_{70}$Ni$_{10}$ (c) and Ni (d) electrodes.

by removing 105 ppm in 24 h (Fig. 5a) corresponding to a conversion yield of 75%. With this cathode, both nitrite and ammonia are produced with a selectivity of 38 and 62%, respectively. At a pure nickel electrode (Fig. 5d), nitrate is exclusively converted to ammonia, but with a conversion yield of only 18% after 24 h. This slow nitrate removal is explained by the poor activity of nickel for nitrate electroreduction, as shown above by the LSV curves, due to the concomitant HER. With cupro-nickel cathodes (Fig. 5b and c), around 100 ppm of nitrate are removed in 24 h with a selectivity of 100% toward ammonia. These results are consistent with our previous work showing that ammonia as the nitrate-reduction product is favored in a potential region close to the HER region, where the reaction between adsorbed hydrogen and adsorbed nitrite to form NH$_3$ may occur [31]. Nickel has an excellent activity for the HER, explaining why this electrode and cupro-nickel materials exclusively produce ammonia as the nitrate electroreduction product.

3.4. Paired electrolysis

Paired electrolyses were carried by using an undivided (i.e., without membrane) multi-cell electrolyzer (Fig. 1) which was based on either Cu, Ni, Cu$_{70}$Ni$_{30}$ or Cu$_{90}$Ni$_{10}$ as cathodes and Ti/IrO$_2$ as anodes. Because nitrate reduction occurs at different potentials depending of the cathode material, it was decided for this investigation to perform electrolysis by controlling the cathode potential. Hence, the electrolysis was performed at a cathode potential of −1.3 V when copper was used, and at −1.1 V when nickel or cupronickel was chosen as cathodes. The anode potential (uncontrolled) was around 1.2–1.5 V during the electrolysis. The current does not vary significantly upon electrolysis and was equal to ca. 6, 7.5, 8.5 and 9 mA cm^{-2} with Ni, Cu$_{70}$Ni$_{30}$, Cu$_{90}$Ni$_{10}$ and Cu cathodes, respectively. The ohmic drop measured by current interruption method was around 0.3 V (for a total cell voltage of ca. 2.3 V).

Fig. 6 shows the evolution of the nitrate concentration as a function of the electrolysis time. During these electrolyses, ammonia was never detected. Moreover, the analysis of nitrate, nitrite, ammonia and N$_2$ provides a mass balance with no significant deficit of N-species. This means that ammonia stripping did not occur during electrolysis and also that chloramines were not significantly produced. This is in agreement with results reported by Vlyssides et al. [38] reporting that chloramine production resulting from the oxidation of ammonia by free chlorine is insignificant at a pH greater than 8. These observations suggest that ammonia was immediately oxidized to nitrogen by chemical oxidation with produced hypochlorite anions. The electrolyses with the Cu$_{70}$Ni$_{30}$ and Cu$_{90}$Ni$_{10}$ cathodes appear to be the most efficient to convert nitrate to nitrogen. After 3 h of electrolysis, the nitrate concentration decreases from 620 to 50 and 88 ppm with the Cu$_{70}$Ni$_{30}$ and
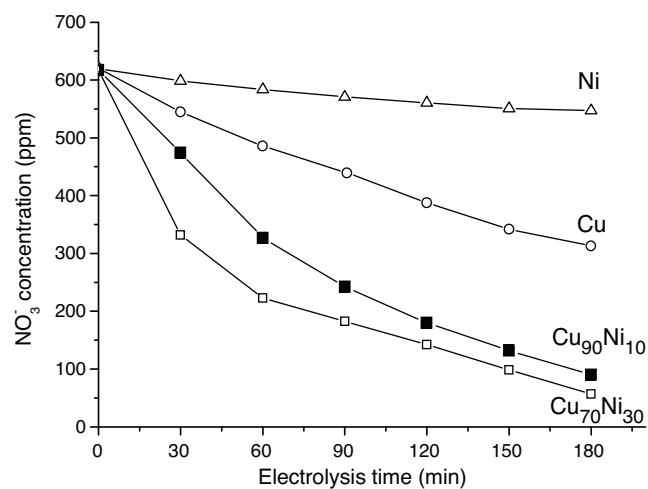

Fig. 6. Evolution of the nitrate concentration during a 3 h paired electrolysis at a cathode potential of −1.3 V with Cu cathodes and −1.1 V with Ni, Cu$_{70}$Ni$_{30}$ and Cu$_{90}$Ni$_{10}$ cathodes in 0.05 M NaCl + 0.01 M NaOH + 0.01 M NaNO$_3$.
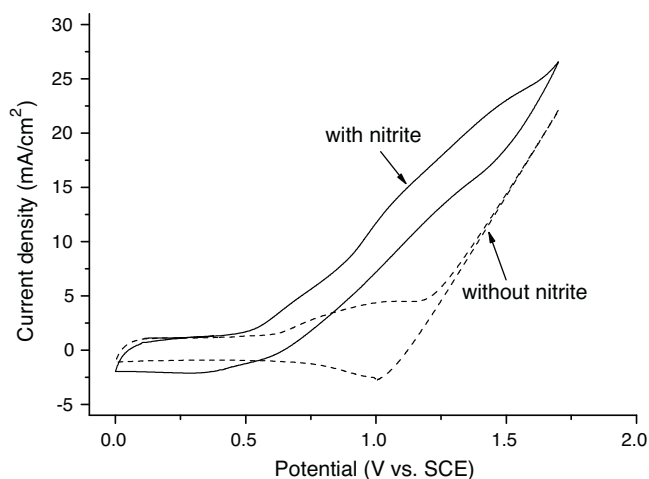
Fig. 7. Cyclic voltammograms of a Ti/IrO$_2$ electrode in 0.5 M NaCl + 0.01 M NaOH without (dashed curve) and with 0.01 M NaNO$_2$ (solid curve). Scan rate: 20 mV s^{-1}.

Cu$_{90}$Ni$_{10}$ cathodes, while it reaches 315 and 540 ppm with copper and nickel cathodes, respectively. The poor paired electrolysis performance with nickel cathodes can be explained by the low activity of these electrodes for nitrate electroreduction as shown previously (Fig. 5). On the other hand, the data of Fig. 5 suggest that the nitrate removal rates with copper and cupro-nickel cathodes should be almost similar. However, during paired electrolysis, the nitrate destruction yield appears smaller when copper is used as the cathode, suggesting that nitrite anions (produced at a pure copper cathode, Fig. 5a) are oxidized at the anode, thus decreasing the overall nitrate elimination rate due to NO$_3^-$ regeneration. This side reaction was confirmed by cyclic voltammetry experiments recorded with a Ti/IrO$_2$ electrode as shown in Fig. 7. In 0.5 M NaCl + 0.01 M NaOH, the curve recorded in the presence of nitrite shows an onset of the anodic current at *ca.* 0.5 V followed by a significant increase of the current, which confirms that nitrite electrooxidation occurs at the Ti/IrO$_2$ electrode. Without nitrite, the cyclic voltammogram is only characterized by an abrupt increase of the anodic current from *ca.* 1.25 V due to the chlorine and oxygen evolution reactions.

Fig. 8 shows the evolution of the specific energy consumption as a function of the paired electrolysis time for the different cathode
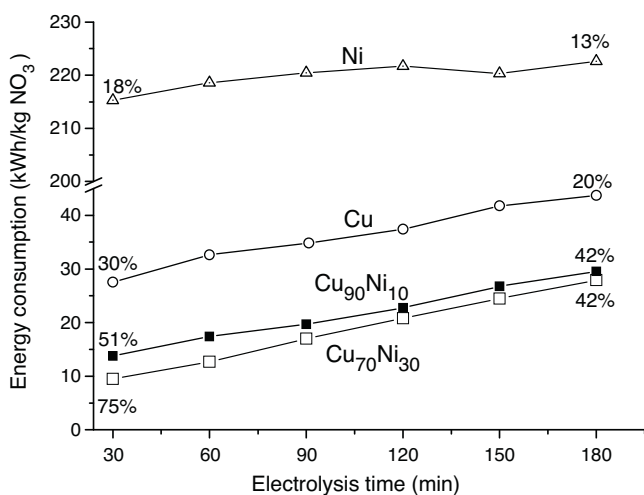

Fig. 8. Evolution of the specific energy consumption during a 3 h paired electrolysis at a cathode potential of −1.3 V with Cu and −1.1 V with Ni, Cu$_{70}$Ni$_{30}$ and Cu$_{90}$Ni$_{10}$ cathodes in 0.05 M NaCl + 0.01 M NaOH + 0.01 M NaNO$_3$. Current efficiencies after 30 and 180 min of electrolysis are also indicated.

materials. It clearly appears that Cu$_{70}$Ni$_{30}$ and Cu$_{90}$Ni$_{10}$ are very effective cathode materials, with a mean energy consumption of only ~20 kWh/kg NO$_3^-$ compared to ~35 and ~220 kWh/kg NO$_3^-$ with pure Cu and Ni cathodes, respectively. In comparison, Cheng et al. [25] reported an energy consumption of 40.1 kWh/kg NO$_3^-$ and a current efficiency for N$_2$ formation of only 24.5% by paired electrolysis in a solid polymer electrolyte reactor with Ti/Pd-Rh and Ti/Pt as cathode and anode materials, respectively. Corbisier et al. reported an energy consumption of 45–71 kWh/kg NO$_3^-$ by paired electrolysis in a two-compartment electrolyzer with copper and Ti/RuO$_2$–TiO$_2$ as cathode and anode materials, respectively [39]. The increase of the specific energy consumption with the electrolysis time observed in Fig. 8 for all materials is due the decrease of the cathodic current efficiency as the nitrate concentration decreases (see below).

Current efficiencies after 30 and 180 min of electrolysis for the different cathode materials are indicated in Fig. 8. By using Cu$_{70}$Ni$_{30}$ cathodes, the CE of the paired electrolysis varies from 75% (after 30 min of electrolysis) to 42% (after 180 min of electrolysis). These CE values are significantly better than those obtained with pure copper (CE ~30–20%) and nickel cathodes (CE ~18–13%). The very low CE with Ni cathodes is due to the high electroactivity of this material for the competitive HER. With a pure copper cathode, HER is less intense but the reoxidation of nitrite to nitrate at the anode, as demonstrated above, reduces the CE of the paired electrolysis. For all cathodes, the CE decreases as the electrolysis time increases. Indeed, during these potentiostatic electrolyses, the current remained almost constant despite the decreasing nitrate concentration, leading to a decrease of the CE. The constant current is mainly due to the HER. The electroreduction of hypochlorite to chloride which occurs at potentials lower than −1 V (confirmed by cyclic voltammetry experiments, not shown) can also decrease the CE, especially for low nitrate/hypochlorite concentration ratios. Consequently, the efficiency (in terms of nitrate removal rate and energy consumption) of the present paired electrolysis process could be improved by adjusting the electrolysis current or the electrode potential as a function of the nitrate concentration in order to favor the reduction of nitrate while limiting the evolution of hydrogen at the cathode and the generation of an excess of hypochlorite at the anode. This point will be studied in detail in a future work.

4. Conclusion

Significant improvement in the nitrate removal by a paired electrolysis process (without membrane) was obtained with a Cu$_{70}$Ni$_{30}$ cathode displaying good corrosion resistance and a high efficiency along with selectivity for the reduction of nitrate to ammonia. Chloride anions were needed to produce hypochlorite at the DSA-type anode, which chemically oxidized ammonia to nitrogen with a 100% selectivity. This process converted nitrate to nitrogen from 620 ppm NO$_3^-$ to 50 ppm NO$_3^-$ with a mean energy consumption as low as 20 kWh/kg NO$_3^-$.

References

[1] S.R. Carpenter, N.F. Caraco, D.L. Correll, R.W. Howarth, A.N. Sharpley, V.H. Smith, Nonpoint pollution of surface waters with phosphorus and nitrogen, Ecol. Appl. 8 (1998) 559–568.
[2] A.H. Wolfe, J.A. Patz, Reactive nitrogen and human health: acute and long-term implications, AMBIO: J. Hum. Environ. 31 (2002) 120–125.

[3] Y.W. Lee, M.F. Dahab, I. Bogardi, Nitrate risk management under uncertainty, J. Water Resour. Plan. Manage. 118 (1992) 151–165.

[4] WHO, Nitrates and Nitrites in Drinking Water, World Health Organization, Geneva, 2004.

[5] K. Rajeshwar, J.G. Ibanez, Environmental Electrochemistry: Fundamentals and Applications in Pollution Abatement, Academic Press, San Diego, CA, 1997.

[6] V. Rosca, M. Duca, M.T. DeGroot, M.T.M. Koper, Nitrogen cycle electrocatalysis, Chem. Rev. 109 (2009) 2209–2244.

[7] C. Milhano, D. Pletcher, The electrochemistry and electrochemical technology of nitrate, Mod. Aspects Electrochem. 45 (2009) 1–61.

[8] H.-l. Li, D.H. Robertson, J.Q. Chambers, D.T. Hobbs, Electrochemical reduction of nitrate and nitrite in concentrated sodium hydroxide at platinum and nickel electrodes, J. Electrochem. Soc. 135 (1988) 1154–1158.

[9] H.L. Li, J.Q. Chambers, D.T. Hobbs, Electroreduction of nitrate ions in concentrated sodium hydroxide solutions at lead, zinc, nickel and phthalocyanine-modified electrodes, J. Appl. Electrochem. 18 (1988) 454–458.

[10] G.E. Dima, A.C.A. De Vooys, M.T.M. Koper, Electrocatalytic reduction of nitrate at low concentration on coinage and transition-metal electrodes in acid solutions, J. Electroanal. Chem. 554–555 (2003) 15–23.

[11] M.C.P.M. Da Cunha, M. Weber, F.C. Nart, On the adsorption and reduction of NO_3^- ions at Au and Pt electrodes studied by in situ FTIR spectroscopy, J. Electroanal. Chem. 414 (1996) 163–170.

[12] K. Bouzek, M. Paidar, A. Sadilkova, H. Bergmann, Electrochemical reduction of nitrate in weakly alkaline solutions, J. Appl. Electrochem. 31 (2001) 1185–1193.

[13] D. Reyter, D. Bélanger, L. Roué, Study of the electroreduction of nitrate on copper in alkaline solution, Electrochim. Acta 53 (2008) 5977–5984.

[14] D. Reyter, G. Chamoulaud, D. Bélanger, L. Roué, Electrocatalytic reduction of nitrate on copper electrodes prepared by high-energy ball milling, J. Electroanal. Chem. 596 (2006) 13–24.

[15] D. Reyter, M. Odziemkowski, D. Bélanger, L. Roué, Electrochemically activated copper electrodes: surface characterization, electrochemical behavior, and properties for the electroreduction of nitrate, J. Electrochem. Soc. 154 (2007).

[16] O. Brylev, M. Sarrazin, D. Bélanger, L. Roué, Rhodium deposits on pyrolytic graphite substrate: physico-chemical properties and electrocatalytic activity towards nitrate reduction in neutral medium, Appl. Catal. B: Environ. 64 (2006) 243–253.

[17] D. Reyter, D. Bélanger, L. Roué, Elaboration of Cu-Pd films by coelectrodeposition: application to nitrate electroreduction, J. Phys. Chem. C 113 (2009) 290–297.

[18] O. Ghodbane, L. Roué, D. Bélanger, Study of the electroless deposition of Pd on Cu-modified graphite electrodes by metal exchange reaction, Chem. Mater. 20 (2008) 3495–3504.

[19] A.C.A. De Vooys, R.A. Van Santen, J.A.R. Van Veen, Electrocatalytic reduction of NO-3 on palladium/copper electrodes, J. Mol. Catal. A: Chem. 154 (2000) 203–215.

[20] J. Chen, H. Shi, J. Lu, Electrochemical treatment of ammonia in wastewater by RuO_2-IrO_2-TiO_2/Ti electrodes, J. Appl. Electrochem. 37 (2007) 1137–1144.

[21] L.L. Xu, H.C. Shi, J.L. Chen, Electrochemical oxidation of ammonia nitrogen wastewater using Ti/RuO_2-TiO_2-IrO_2-SnO_2 electrode, Huanjing Kexue/Environ. Sci. 28 (2007) 2009–2013.

[22] K.W. Kim, Y.J. Kim, I.T. Kim, G.I. Park, E.H. Lee, Electrochemical conversion characteristics of ammonia to nitrogen, Water Res. 40 (2006) 1431–1441.

[23] K.W. Kim, I.T. Kim, G.I. Park, E.H. Lee, Electrolytic decomposition of ammonia to nitrogen in a multi-cell-stacked electrolyzer with a self-pH-adjustment function, J. Appl. Electrochem. 36 (2006) 1415–1426.

[24] Y. Vanlangendonck, D. Corbisier, A. Van Lierde, Influence of operating conditions on the ammonia electro-oxidation rate in wastewaters from power plants (ELONITA technique), Water Res. 39 (2005) 3028–3034.

[25] H. Cheng, K. Scott, P.A. Christensen, Paired electrolysis in a solid polymer electrolyte reactor—simultaneously reduction of nitrate and oxidation of ammonia, Chem. Eng. J. 108 (2005) 257–268.

[26] J. Yu, M.J. Kupferle, Two-stage sequential electrochemical treatment of nitrate brine wastes, Water Air Soil Pollut.: Focus 8 (2008) 379–385.

[27] M. Li, C. Feng, Z. Zhang, N. Sugiura, Efficient electrochemical reduction of nitrate to nitrogen using Ti/IrO_2-Pt anode and different cathodes, Electrochim. Acta 54 (2009) 4600–4606.

[28] M. Li, C. Feng, Z. Zhang, S. Yang, N. Sugiura, Treatment of nitrate contaminated water using an electrochemical method, Bioresour. Technol. 101 (2010) 6553–6557.

[29] L. Szpyrkowicz, S. Daniele, M. Radaelli, S. Specchia, Removal of NO_3^- from water by electrochemical reduction in different reactor configurations, Appl. Catal. B: Environ. 66 (2006) 40–50.

[30] D. Corbisier, L. Vereist, Y. Vanlangendonck, A. Van Lierde, Electro-degradation of nitrate ions and ammonia from power station effluents the ELONITA technique, VGB PowerTech 86 (2006).

[31] D. Reyter, D. Bélanger, L. Roué, Nitrate removal by a paired electrolysis on copper and Ti/IrO_2 coupled electrodes—influence of the anode/cathode surface area ratio, Water Res. 44 (2010) 1918–1926.

[32] L.J. Korb, D.L. Olson, Corrosion Metals Handbook, vol. 13, 9th ed., 1987, p. 677.

[33] L. Durivault, O. Brylev, D. Reyter, M. Sarrazin, D. Bélanger, L. Roué, Cu–Ni materials prepared by mechanical milling: their properties and electrocatalytic activity towards nitrate reduction in alkaline medium, J. Alloys Compd. 432 (2007) 323–332.

[34] K.M. Ismail, A.M. Fathi, W.A. Badawy, The influence of Ni content on the stability of copper–nickel alloys in alkaline sulphate solutions, J. Appl. Electrochem. 34 (2004) 823–831.

[35] A.M. Zaky, F.H. Assaf, Cyclic voltammetric behaviour of copper–nickel alloys in alkaline media, Br. Corros. J. 37 (2002) 48–55.

[36] A. Al-Hashem, J. Carew, The use of electrochemical impedance spectroscopy to study the effect of chlorine and ammonia residuals on the corrosion of copper-based and nickel-based alloys in seawater, Desalination 150 (2002) 255–262.

[37] J.N. Alhajji, M.R. Reda, On the effects of common pollutants on the corrosion of copper–nickel alloys in sulfide polluted seawater, J. Electrochem. Soc. 142 (1995) 2944–2953.

[38] A.G. Vlyssides, P.K. Karlis, N. Rori, A.A. Zorpas, Electrochemical treatment in relation to pH of domestic wastewater using Ti/Pt electrodes, J. Hazard. Mater. 95 (2002) 215–226.

[39] D. Corbisier, Y. Vanlangendonck, A. Van Lierde, Electrochemical device and method for the removal of ammonium and nitrate ions contained in liquid effluents. Int. Patent WO/2005/097686 (2005).